Geophysical Journal International

Geophys. J. Int. (2012) **189,** 161–168 doi: 10.1111/j.1365-246X.2012.05397.x

Anatomy of the Andean subduction zone: three-dimensional density model upgraded and compared against global-scale models

Andrés Tassara and Andrés Echaurren

Departamento de Ciencias de la Tierra, Facultad de Ciencias Químicas, Universidad de Concepción, Victor Lamas 1290*, Barrio Universitario, Casilla* 160-C*, Concepción, Chile. E-mail: andrestassara@udec.cl*

Accepted 2012 January 27. Received 2012 January 3; in original form 2011 March 3

SUMMARY

We present an upgraded version of a previously published 3-D density model of the Andean subduction zone between 18°S and 45°S. This model consists of 3-D bodies of constant density, which geometry is constrained by independent seismic data and is triangulated from vertical cross-sections. These bodies define the first-order morphology and internal structure of the subducted Nazca slab and South American Plate. The new version of the density model results after forward modelling the Bouguer anomaly as computed from the most recent version of the Earth Gravitational Model (EGM2008). The 3-D density model incorporates new seismic information to better constrain the geometry of the subducted slab and continental Moho (CMH) and has a trench-parallel resolution doubling the resolution of the previous model. As an example of the potential utility of our model, we compare the geometry of the subducted slab and CMH against the corresponding global models Slab1.0 and Crust2.0, respectively. This exercise demonstrates that, although global models provide a good first-order representation of the slab and upper-plate crustal geometries, they show large discrepancies (up to ±40 km) with our upgraded model for some well-constrained areas. The geometries of the slab, lithosphere–asthenosphere boundary below the continent, CMH and intracrustal density discontinuity that we present here as Supporting Information can be used to study Andean geodynamic processes from a wide range of quantitative approaches.

Key words: Gravity anomalies and Earth structure; Subduction zone processes; South America.

1 INTRODUCTION

The Chilean margin along the southwestern coast of South America (SA) is the type locality of strongly compressive subduction zones (Uyeda & Kanamori 1979; Heuret & Lallemand 2005). Plate convergence between Nazca (NZ) and SA occurs at rates of 66 mm yr^{-1} in a nearly perpendicular direction with respect to the NS-oriented trench axis (Kendrick *et al.* 2003; Ruegg *et al.* 2009). Rapid convergence is partially absorbed as crustal shortening and thickening to produce the largest non-collisional orogen on the Earth, the Andes Cordillera (Isacks 1988; Oncken *et al.* 2006). Long-term dynamic support of the Andes requires elevated shear strength along the interplate seismogenic zone (Yáñez & Cembrano 2004; Lamb 2006), which leads to the largest megathrust earthquakes on the planet. The geometry of the subducted slab changes along the margin between normally dipping (30°) and subhorizontal (<10°; Cahill & Isacks 1992), controlling the locus of magmatic chains and volcanic gaps (Stern 2004). A better understanding of this rich range of geodynamic processes can be gained if sufficient knowledge is provided on the current anatomy, that is, 3-D structure, of the Andean margin.

Here we present an upgraded version of the 3-D density model of the NZ Plate and the Andean margin published by Tassara *et al.* (2006, hereafter T06). T06 model was constructed by forward modelling the Bouguer gravity anomaly under the constraints of published geophysical data and is a continental-scale representation of the internal structure of NA and SA plates. Electronic material accompanying T06 has been used for a number of quantitative approaches. This includes the complementation of isotopic data for the delineation of crustal domains at the Central Andes (Mamani *et al.* 2008), characterization of continental lithosphere thickness and comparison against the elastic thickness (Pérez-Gussinyé *et al.* 2008), constraining the 3-D forearc structure below a first-order seismic segment boundary (Melnick *et al.* 2009), prediction of the rheological stratification of the lithosphere contributing to the understanding of Andean mountain building processes (Farías *et al.* 2010), computation of vertical stresses loading the Chilean megathrust with implications for the recognition of seismic asperities (Tassara 2010) and the definition of geometries for a 3-D finite element model that has been applied to estimate coseismic slip distribution for the M_w9.5 1960 Valdivia Earthquake (Moreno *et al.* 2009) and pre-seismic locking before the M_w8.8 2010 Maule Earthquake (Moreno *et al.* 2010).

In this upgraded version of the 3-D density model of the NZ Slab and Andean margin we increased the along-strike resolution of the

model with respect to T06, using a high-resolution and spatially continuous Bouguer anomaly computed from the Earth Gravitational Model 2008 (Pavlis *et al.* 2008) and incorporating seismic constraints published after the creation of T06. We describe methods, data and results obtained after this upgrading. As an example of the utility of our well-constrained model, we compare the new geometries of the slab and continental crust against global-scale models to show that such models are good first-order representations but they fail describing important details of the Andean structure. We think that geometries for the slab upper surface, continental lithosphere–asthenosphere boundary (LAB), continental Moho (CMH) and intracrustal discontinuity (ICD) that we present here as Supporting Information will be of usefulness for a number of quantitative applications related to short- and long-term geodynamic, tectonic and seismogenic processes occurring inside the Andean margin.

2 METHOD

To describe the distribution of masses inside the Andean subduction zone between 5°S and 45°S, the T06 model considers a number of 3-D bodies to represent the density structure of the oceanic NZ Plate, subducted slab and overriding South American Plate (Fig. 1). A constant value of density is assigned to each of these bodies based on petrophysical considerations that take into account the expected lateral variations of composition and pressure–temperature conditions below the margin [Fig. 1; see details of the model design and assignation of density values in Tassara *et al.* (2006)]. The 3-D density structure of T06's model was triangulated from 43 vertical cross-sections that are parallel to the convergence direction and separated by one geographic degree between them. For each cross-section, the model visually integrates available sources of geophysical data to constraint the geometry of first-order density discontinuities like the slab upper surface, the LAB below the continental plate, the CMH and an ICD that separates upper (light) and lower (dense) crustal bodies. The gravity effect of the triangulated 3-D density structure is computed following a formulation described elsewhere (Goetze & Lahmeyer 1988) and then visually compared along each section against the observed Bouguer anomaly. By iteratively changing the position of vertices that form density discontinuities for each section in accordance to independent geophysical information, the selected final model produces the best possible fit between the observed and computed Bouguer anomaly. The along-strike (trench-parallel) resolution of the T06 model is limited to half of the distance between each cross-sections (~50 km), whereas

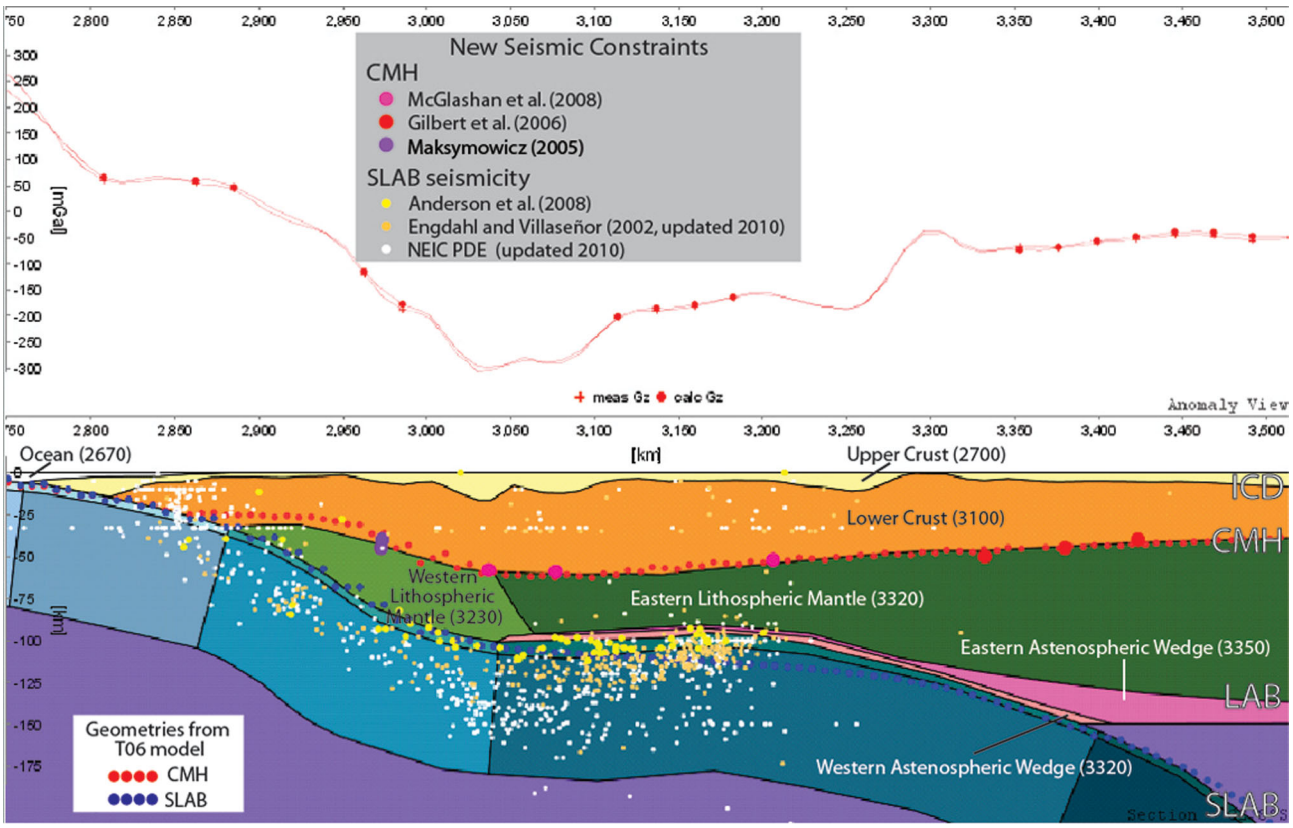

Figure 1. Cross-section of the 3-D density model. This section intersects the trench axis at 32.8°S, runs parallel to the convergence direction and is shown as an example of the IGMAS software that was used to construct the present model. Upper panel: curves for the measured (meas Gz) and model-calculated (calc Gz) Bouguer anomaly, which almost coincide along this section (as for the rest of the model). Lower panel: it shows the structure of the density model as formed by different bodies of constant density (each with a different colour). Values of density for bodies forming the upper plate are shown in parenthesis in units of kg m^{-3}. Values of density for the subducted slab are not shown because they change from north to south in accordance to variations in the slab age at the trench (see Tassara *et al.* 2006 for details). The right-hand part shows the acronyms and definition for the slab upper surface (SLAB), continental lithosphere–asthenosphere boundary (LAB), continental Moho (CMH) and intracrustal discontinuity (ICD). The figure includes new seismic constraints for the CMH and SLAB contained as points in the compiled database (see references in the legend of the upper panel) that were used to modify the geometries of these discontinuities with respect to those of the T06 model (legend in the lower panel).

the across-strike resolution is higher because short-wavelength features (∼10 km) of the Bouguer anomaly are directly fitted for each section.

The new version of the model was constructed using a recent edition of the Interactive Gravity and Magnetic Application System (IGMAS, http://www.gravity.uni-kiel.de/igmas/). It has the same east–west length than that one in T06 model (85–60°W) but covers only the Chilean part of the NZ–SA convergent margin between 18°S and 45°S. This upgraded version is constructed by triangulation between 55 vertical cross-sections that are oriented following the convergence direction (as for the T06 model) and are separated by 0.5° in latitude. Thus, the along-strike resolution is now 25 km, doubling the resolution of T06's model.

3 DATA

3.1 Bouguer anomaly

Gravity data used by the T06 model is a compilation of point measurements inland and altimetry-derived marine gravity data that were used to compute the simple Bouguer anomaly (i.e. without terrain corrections) following standard procedures (Blakely 1996) and tied to the WGS84 reference ellipsoid. For this upgraded version of the 3-D density model we use the release 2008 of the Earth Gravitational Model (EGM2008; Pavlis *et al.* 2008). The EGM2008 model is an optimized combination of available land data, marine gravity from satellite altimetry and data obtained by the Gravity Recovery And Climate Experiment (GRACE) satellite mission. The EGM2008 model has been released as a spherical harmonic representation and is complete until degree and order 2159, meaning a spatial resolution of *ca.* 10 km. From the International Center for Global Earth Models (http://icgem.gfz-potsdam.de/ICGEM/ICGEM.html) we downloaded the so-called classical gravity anomaly computed by ICGEM from EGM2008 with reference to the WGS84 ellipsoid, ensuring its direct comparison with the T06 gravity database. This corresponds to the free air anomaly computed at the ellipsoid surface, from which we then calculated the simple Bouguer anomaly following a procedure described elsewhere (Tassara *et al.* 2007); this considers computing a simple Bouguer correction from GEBCO topography/bathymetry data (http://www.ngdc.noaa.gov/mgg/gebco/gebco.html) using an infinite slab with density 2670 kg m^{-3} onshore and 1650 kg m^{-3} offshore. The Bouguer corrections were low-pass filtered with a cut-off wavelength of 20 km, which ensures that short-wavelength noise due to a rough topography will not be introduced into the calculated Bouguer anomalies. Terrain corrections were not included to produce a simple Bouguer anomaly comparable with the one used in the T06 model.

We produce a regular Bouguer anomaly grid for the area of study with a spatial resolution of 5 km, that is, forcing the EGM2008 model to half of its maximum spatial resolution. The error in the free-air gravity anomaly estimated for EGM2008 varies with wavelength but reaches 5–10 mGal at the maximum degree and order used here (Pavlis *et al.* 2008).

Fig. 2 shows differences between Bouguer anomaly values contained in T06's database and the EGM2008-derived grid used here. This map shows the irregular and locally poor spatial distribution of land gravity stations used by the T06 model. Although the public documentation of EGM2008 does not describe the origin and distribution of land data included on it, this model likely considers the same data used by T06 for the Andean region, which were those gravity data publically available at the time of publication. Therefore, the small difference observed in Fig. 2 between T06 and EGM2008 for most of the onshore Andean margin is to be expected. For high-topography regions of the central Andes where land gravity data were not included in the T06 database and probably are also lacking in EGM2008, Bouguer anomalies are mostly derived from a topography-based prediction of gravity and complemented with GRACE observations at long wavelengths (Pavlis *et al.* 2008). This means that there are still relatively large uncertainties in the gravity field at short wavelengths (<50 km) for such regions. Nevertheless, we preferred to use the EGM2008 in our study because it allows a spatially continuous and regular representation of the Bouguer anomaly for the entire area of interest. Fig. 2 remarks that for most of the study area the differences between old and new gravity data are lower than the average error in the Bouguer anomaly reported by T06 (±20 mGal). For areas where the difference is larger than this value, the upgraded density structure must be modified with respect to that one considered by the T06 model to compensate changes in the observed gravity field.

3.2 Seismic data

We compiled relevant seismic information published after the creation of the T06 model (mid 2005), which is used to further constraint the geometry of the subducted slab and CMH (Figs 1 and 2). For the slab geometry we added to the previous seismicity database new hypocentre determinations from temporal, local seismic networks (Anderson *et al.* 2007; Lange *et al.* 2007; Haberland *et al.* 2009) that complement teleseismic location hypocentre information from updated versions (end 2010) of the Centennial Catalogue (Engdahl & Villaseñor 2002) and the National Earthquake and Information Center (NEIC) Preliminary Determination of Epicenter (PDE) catalogue. We also digitized the upper surface of the slab as imaged by active source seismic profiles (Sallares & Ranero 2005; Krawczyk *et al.* 2006; Contreras *et al.* 2008; Scherwath *et al.* 2009; Moscoso *et al.* 2011) and modified the geometry of the crust–mantle boundary adding new constraints from receiver function studies (Maksymowicz 2005; Gilbert *et al.* 2006; Heit *et al.* 2008; Woelbern *et al.* 2009; Perarnau *et al.* 2010) and teleseismically recorded Moho reflections (McGlashan *et al.* 2008). Fig. 1 shows one modelling cross-section extracted from the original IGMAS model as an example of how this seismic information is used to constraint and modify the geometry of the slab upper surface and the CMH.

4 RESULTS

The final geometries for the slab upper surface (SLAB), continental LAB, CMH and ICD that resulted after this upgrading are presented as Supporting Information in the form of ASCII tables that contain the position (longitude, latitude and depth below sea level) of vertices defining each discontinuity across the modelled sections. Using the adjustable tension continuous curvature surface gridding algorithm of the Global Mapping Tools (Wessel & Smith 1991), we interpolate these vertices into regular and continuous grids of 5 × 5 km cell size to produce maps showing the topography of each discontinuity below the Andean margin (Figs 3A–D). Depths uncertainties arise from original uncertainties in the geophysical information used to constraint each discontinuity (as discussed by T06) and produce average values of 10 km for SLAB and LAB, 5 km for CMH and 2 km for ICD. These uncertainties do not consider

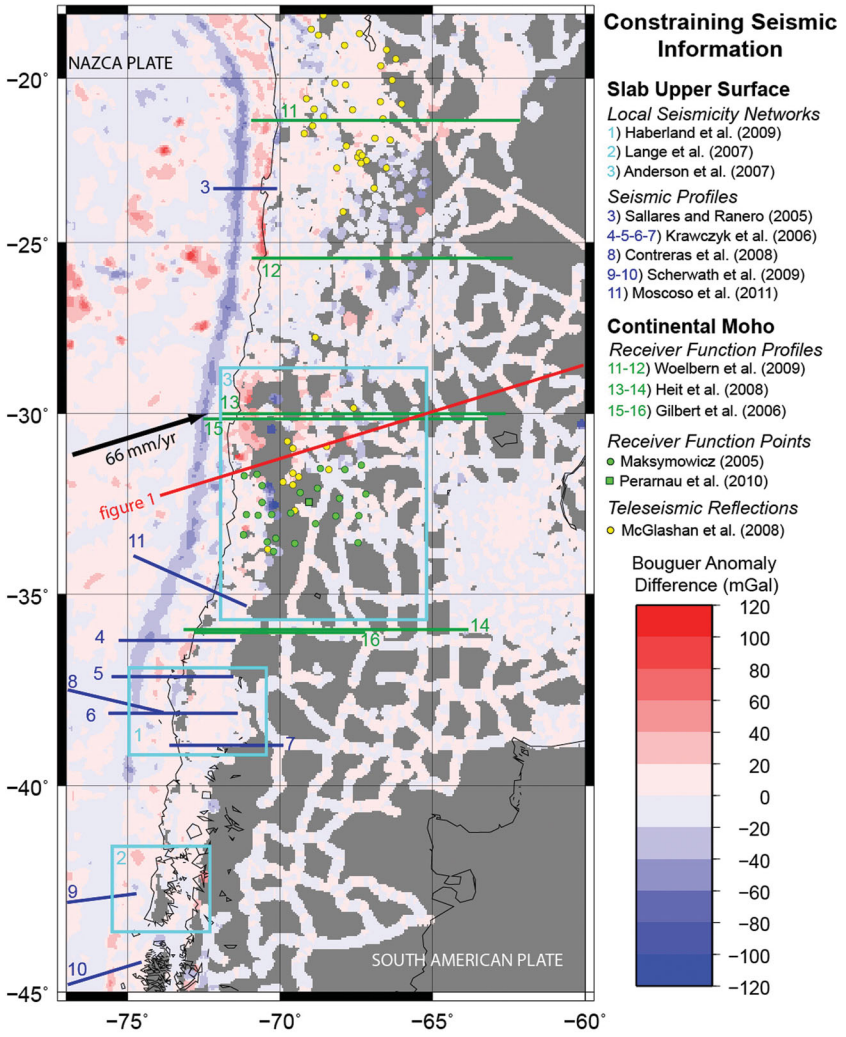

Figure 2. New gravity and seismic data. The map is a representation of a 5 × 5 km grid of the studied region that have values only for nodes containing at least one gravity station of those considered for the Tassara *et al.* (2006; T06 model) database inside a radius of 15 km. These nodes are colour coded according to the difference between Bouguer anomaly values reported by T06 model and values computed from the 2008 version of the Earth Gravitational Model (Pavlis *et al.* 2008), which is used here. Squares, lines and circles show the location of seismic data added to the T06 database during the present upgrading. Black arrow shows current convergence velocity vector (Kendrick *et al.* 2003). Red line shows the location of cross-section of Fig. 1.

the fact that terrain corrections were not applied in the computation of the Bouguer anomaly for both models. Terrain corrections for regions of the Andean margin characterized by an extremely high relief (e.g. near the coast of northern Chile, Eastern Cordillera of Bolivia and eastern flank of the Frontal Cordillera in Argentina) can contribute maximum values of 10–25 mGal (Goetze & Kirchner 1997). These values are inside the general error of the gravity anomaly assumed by T06 model but are larger than the error of the EGM2008-derived Bouguer anomaly used in this new version. Considering that the SLAB, LAB and CMH geometries are mostly constrained by independent seismic information, errors in the Bouguer anomaly caused by avoiding terrain corrections would translate into further uncertainties in the ICD geometry. Following the sensitivity analysis presented by Tassara *et al.* (2006), this will imply that the depth to the ICD in our model can be overestimated by up to 3 km for high-relief regions at local scales. Future versions of the model will incorporate terrain corrections in the computation of the complete Bouguer anomaly to reduce sources of uncertainties and errors in the final geometry of the ICD at local scales. Nevertheless, we think that the regional-scale tendency of the ICD would not change compared to this present version.

To better appreciate changes incorporated to these geometries during the present upgrading, we compute the depth difference between new and old geometries for every vertex of each discontinuity of the upgraded model, and produce discrete grids from them (Figs 3E–H). Regional changes in the geometry of SLAB are larger than its uncertainty below the southern Chile forearc (around 74°W; 43°S) where new seismic data show that the slab is 15–25 km deeper than estimated by T06's model, and for the Argentinean flat-slab (around 68°W; 30°S) where newly incorporated seismicity from local-to-regional studies imposes 10–20 km shallower depths of the slab. Because no additional information has been incorporated to constrain the LAB geometry, it shows no significant changes other than some variations introduced to follow changes on SLAB and CMH. New seismic constraints for the CMH impose notable deepening (up to 20 km) below the northernmost and south-central Chile forearc and a shallowing (5–10 km) in areas eastwards of these regions. Variations in the subcrustal mass distribution generated by

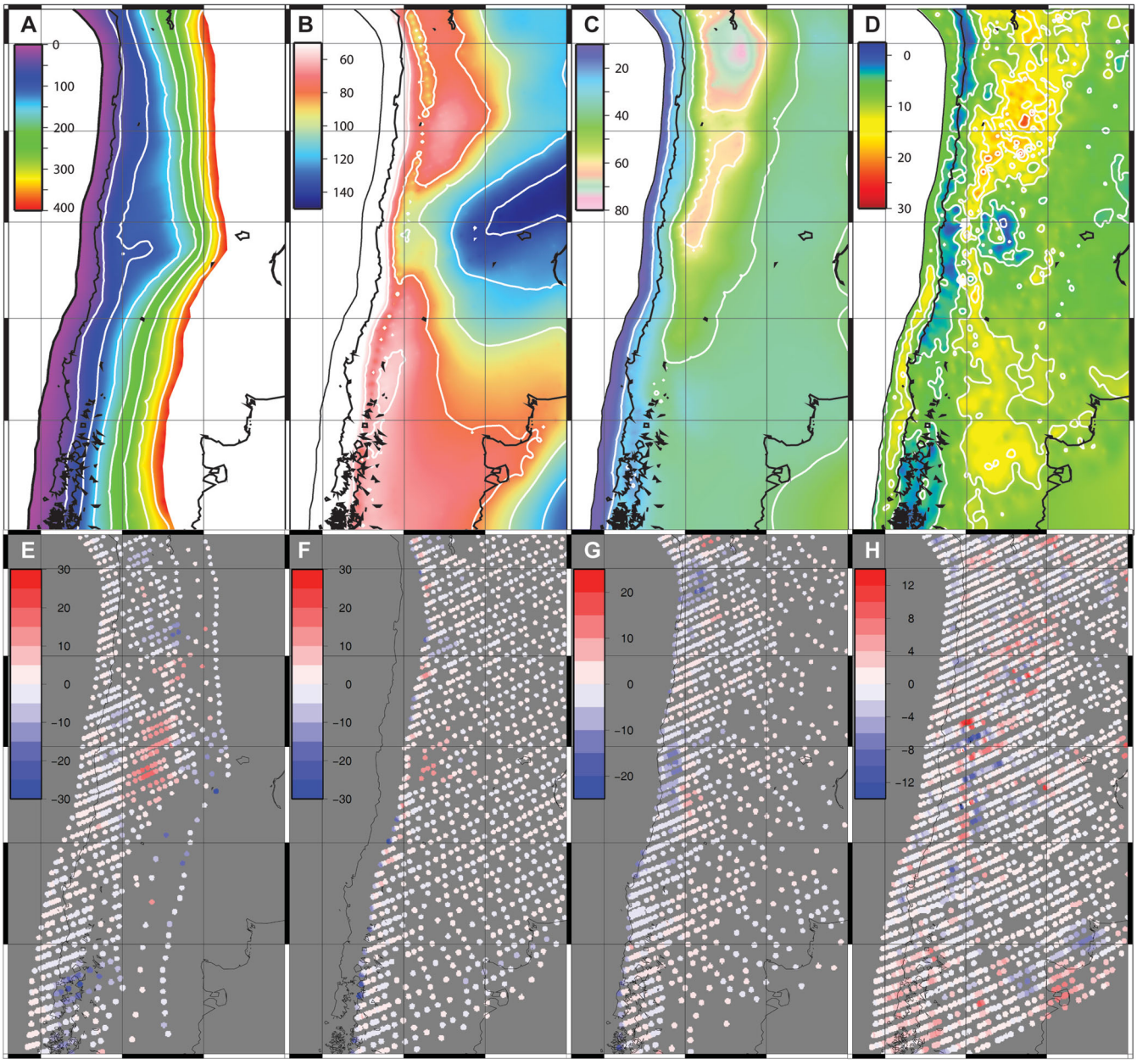

Figure 3. Upgraded geometries of the 3-D density model. Upper panel (A–D): map representation of continuous 5 × 5 km grids constructed from vertices defining the depth from the sea level to the slab upper surface SLAB (A), lithosphere–asthenosphere boundary (LAB) (B), continental Moho (CMH) (C) and intracrustal discontinuity (ICD) (D). Lower panel (E–H): maps showing the location of these vertices as colour coded by the difference in the depth to each discontinuity between T06 model and this upgraded version. A positive difference (red) indicates an overestimation for the depth to the corresponding discontinuity of the T06 model with respect to the present model. All colour scales are in kilometres.

changes in SLAB, LAB and CMH geometries are compensated in terms of the forward gravity modelling by reciprocal changes in the ICD geometry. However, large amplitude (>10 km absolute value) and short-wavelength (<20 km) difference between old and new ICD geometries are mostly due to differences between Bouguer anomaly data used for both versions of the model. This is most notable along the high cordilleran region of central Chile and Argentine where T06 model had no gravity data, the EGM2008 gravity model is relatively less confidential and terrain corrections are likely the largest; therefore, the ICD geometry here should be considered and interpreted with caution.

5 COMPARISON AGAINST GLOBAL-SCALE MODELS

We further compare the new SLAB and CMH geometries against estimates of the global-scale models Slab1.0 (Hayes *et al.* 2012) and Crust2.0 (Bassin *et al.* 2000) to test the ability of these models for describing the 3-D structure of the Andean margin. This comparison (Fig. 4) is shown here as an example of the kind of analysis that is possible with our well-constrained model.

Fig. 4(A) shows depth differences between our SLAB grid and point estimates of the depth to the slab upper surface contained

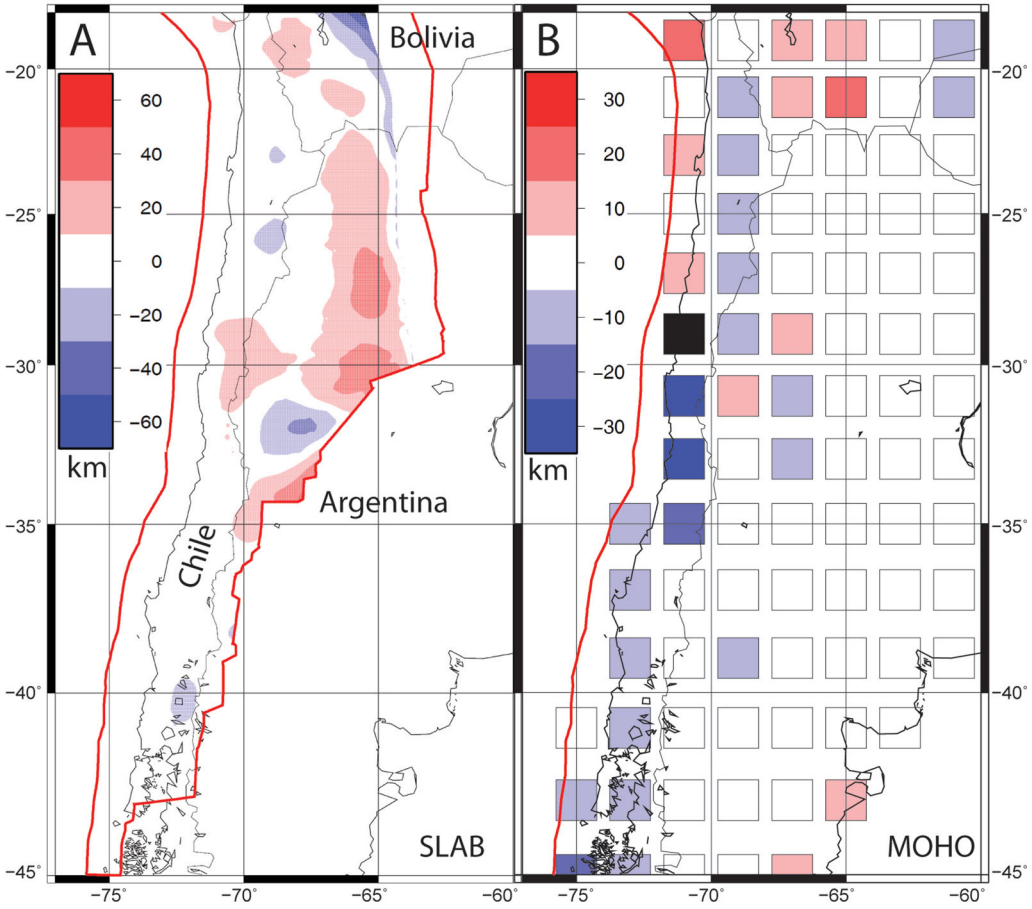

Figure 4. Comparison with global-scale models. Depth differences between geometries of the upgraded model compared to (A) the slab depth from Slab1.0 (Hayes *et al.* 2012) and (B) continental Moho depth from Crust2.0 (Bassin *et al.* 2000). A positive difference (red) indicates an overestimation for the depth to the corresponding discontinuity of the global models with respect to the present model. Colour scales are in kilometres. Red line shows the extent of Slab1.0 model in (A) and the location of the trench axis in (B).

in the ASCII table sam_slab1.0_clip.xyz available from the Slab1.0 website (http://earthquake.usgs.gov/research/data/slab). For most of the studied region, both models agree between a 10 km uncertainty limit. This is particularly true below the Chilean forearc where Slab1.0 makes a good job describing the megathrust geometry (which is the main goal of this global model), even considering that it does not include several of the seismic data incorporated in our model (Anderson *et al.* 2007; Lange *et al.* 2007; Contreras *et al.* 2008; Moscoso *et al.* 2011). However, Slab1.0 overestimates by a large magnitude (10–40 km) the depth to the slab in the Argentinian flat-slab region in comparison to our modelling where refined seismicity estimations from local seismic studies (Anderson *et al.* 2007) combined with recent teleseismic data are included. The large positive difference below northwestern Argentina, where almost no seismicity is recorded at 200–400 km depth by teleseismic catalogues used by both models, is due to the fact that Slab1.0 prefers a larger upward convexity than our model to link intermediate-depth (<200 km) and deep (>550 km) seismicity.

Fig. 4(B) depicts depth difference between our CMH grid and estimates of the CMH depth contained in the gridded ASCII file map2.t7.gmt available from the Crust2.0 website (http://igppweb.ucsd.edu/ğabi/rem.html). This model is based on a compilation of active seismic profiles that is used in combination to the age and tectonic regimen of a given region to assign types of crustal structure to grid nodes at a 2° × 2° resolution covering the entire Earth. For most of the planet where no seismic profiles are directly used (the case of SA), Crust2.0 can be considered a prediction of the crustal structure. Fig. 4(B) shows that this prediction, although very coarse in resolution, is quite good for most of the nodes that cover our model region, particularly below Argentina where both models coincide between a 5 km uncertainty limit. However, the Moho depth of Crust2.0 is 10–25 km lower than our estimate below the extremely thick (75–80 km) and good-constrained Bolivian Altiplano Crust. Moreover, the largest discrepancies are notable below the Chilean side of the margin, where Crust2.0 either underestimate crustal depths (offshore region between 18°S and 27°S) or overestimates the depth to the Moho, reaching differences with our model as large as 25–40 km (29°S and 33°S). These large differences in the forearc region, where we use several seismic constraining data, could be explained because the crustal structure here is intrinsically complicated by the intersection of the continental margin and the slab along the subduction interface. Our study shows that paying attention to the details of subduction zone structure should improve new versions of global crustal models.

6 CONCLUDING REMARKS

This upgraded version of the gravity-derived 3-D density model of the Andean margin integrates most of the seismic data reported in the literature in a unified and well-constrained continental-scale

representation of the internal anatomy below the margin. This model can be useful for a number of applications, and we showed here an example by comparing geometries of the model against those of global-scale models for the subducted slab and continental crust. This exercise showed that Slab1.0 (Hayes *et al.* 2012) and Crust2.0 (Bassin *et al.* 2000) models give a good first-order representation of the geometries of the slab upper surface and the depth to the CMH, particularly for the megathrust interplate fault below the Chilean forearc in the case of Slab1.0 and the stable Argentinean foreland for Crust2.0. However, large discrepancies do exist for several regions where we included local seismic estimations as constraining data input for our modelling. These results could be valuable for authors of these global-scale models during future construction of improved versions and for other researchers that would like to have an independent estimate of the quality and performance of these global models in comparison with better constrained representations of the internal Earth structure. We hope that the Andean geoscientific community interested in the study of short- and long-term processes from a quantitative perspective could further benefit from this upgraded version of the model and the electronic geometries of SLAB, LAB, CMH and ICD that are available as Supporting Information with this article.

ACKNOWLEDGMENTS

This work was supported by Chilean FONDECYT projects 1070279 ACHISZS (Anatomy of the CHIlean Subduction Zone and Seismogenesis) and 1101034 CONPARSA (CONvergence PARtitioning at the Southern Andes). We thank the reviews of Patricia Alvarado and Sylvain Bonvalot and comments of the Editor Michel Diament that greatly improved the clarity and quality of this paper.

REFERENCES

Anderson, M., Alvarado, P., Zandt, G. & Beck, S., 2007. Geometry and brittle deformation of the subducting Nazca Plate, Central Chile and Argentina, *Geophys. J. Int.,* **171,** 419–434.

Bassin, C., Laske, G. & Masters, G., 2000. The current limits of resolution for surface wave tomography in North America, *EOS, Trans. Am. geophys. Un.,* **81,** 897.

Blakely, R., 1996. *Potential Theory in Gravity and Magnetic Applications,* 2nd edn, Cambridge University Press, Cambridge.

Cahill, T. & Isacks, B.L., 1992. Seismicity and shape of the subducted Nazca Plate, *J. geophys. Res.,* **97,** 17 503–17 529.

Contreras, E., Grevemeyer, I., Flueh, E.R. & Reichert, C., 2008. Upper lithospheric structure of the subduction zone offshore of southern Arauco peninsula, Chile, at 38°S, *J. geophys. Res.,* **113,** doi:10.1029/2007JB005569.

Engdahl, E.R. & Villaseñor, A., 2002. 41 Global seismicity, in *International Handbook of Earthquake and Engineering Seismology,* pp. 665–690, eds Lee, W., Kanamori, H., Jennings, P. & Kisslinger, C., Academic Press, London.

Farías, M., Comte, D., Charrier, R., Martinod, J., David, C., Tassara, A., Tapia, F. & Fock, A., 2010. Crustal-scale structural architecture in central Chile based on seismicity and surface geology: implications for Andean mountain building, *Tectonics,* **29,** doi:10.1029/2009TC002480.

Gilbert, H., Beck, S. & Zandt, G., 2006. Lithospheric and upper mantle structure of central Chile and Argentina, *Geophys. J. Int.,* **165,** 383–398.

Goetze, H.-J. & Kirchner, A., 1997. Interpretation of gravity and geoid in the central Andes between 20° and 29°S, *J. South Am. Earth Sci.,* **10,** 179–188.

Goetze, H.-J. & Lahmeyer, B., 1988. Application of three-dimensional interactive modeling in gravity and magnetics, *Geophysics,* **53,** 1096–1108.

Haberland, C., Rietbrock, A., Lange, D., Bataille, K. & Dahm, T., 2009. Structure of the seismogenic zone of the southcentral Chilean margin revealed by local earthquake traveling tomography, *J. geophys. Res.,* **114,** doi:10.1029/2008JB005802.

Hayes, G.P., Wald, D. & Johnson, R., 2012. Slab1.0: A three dimensional model of global subduction zone geometries, *J. geophys. Res.,* **117,** doi:10.1029/2011JB008524.

Heit, B., Yuan, X., Bianchi, M., Sodouri, F. & Kind, R., 2008. Crustal thickness estimation beneath the southern central Andes at 30°S and 36°S from S wave receiver function analysis, *Geophys. J. Int.,* **174,** 249–254.

Heuret, A. & Lallemand, S., 2005. Plate motions, slab dynamics and back-arc deformation, *Phys. Earth planet. Inter.,* **149,** 31–51.

Isacks, B.L., 1988. Uplift of the central Andean Plateau and bending of the Bolivian Orocline, *J. geophys. Res.,* **93,** 3211–3231.

Kendrick, E., Bevis, M., Smalley Jr., R., Brooks, B., Vargas, R.C., Lauría, E. & Fortes, L.P.S., 2003. The Nazca-South America Euler vector and its rate of change, *J. South Am. Earth Sci.,* **16,** 125–131.

Krawczyk, C. *et al*., 2006. Geophysical signatures and active tectonics at the south-central Chilean margin, in *The Andes: Active Subduction Orogeny,* pp. 171–192, eds Oncken, O., Chong, G., Franz, G., Giese, P., Götze, H.-J., Ramos, V. A., Strecker, M. & Wigger, P., Springer-Verlag, Berlin.

Lamb, S., 2006. Shear stresses on megathrusts: implications for mountain building behind subduction zones, *J. geophys. Res.,* **111,** doi:10.1029/2005JB003916.

Lange, D., Rietbrock, A., Haberland, C., Bataille, K., Dahm, T., Tilmann, F. & Flueh, E.R., 2007. Seismicity and geometry of the south Chilean subduction zone (41.5°S-43.5°S): implications for controlling parameters, *Geophys. Res. Lett.,* **34,** doi:10.1029/2006GL029190.

Maksymowicz, A., 2005. Modelo 3D del Moho bajo la zona de Chile central y oeste de Argentina (31°S–34°S), utilizando funciones de recepción, Magister en Ciencias, mención Geofísica, Universidad de Chile, Santiago, Chile.

Mamani, M., Tassara, A. & Woerner, G., 2008. Composition and structural control of crustal domains in the central Andes, *Geochemist. Geophys. Geosyst.,* **9,** doi:10.1029/2007GC001925.

McGlashan, N., Brown, L. & Kay, S., 2008. Crustal thickness in the central Andes from teleseismically recorded depth phase precursors, *Geophys. J. Int.,* **175,** 1013–1022.

Melnick, D., Bookhagen, B., Strecker, M. & Echtler, H., 2009. Segmentation of megathrust rupture zones from fore-arc deformation patterns over hundreds to millions of years, Arauco peninsula, Chile, *J. geophys. Res.,* **114,** doi:10.1029/2008JB005788.

Moreno, M., Bolte, J., Klotz, J. & Melnick, D., 2009. Impact of megathrust geometry on inversion of coseismic slip from geodetic data: application to the 1960 Chile earthquake, *Geophys. Res. Lett.,* **36,** doi:10.1029/2009GL039276.

Moreno, M., Rosenau, M. & Oncken, O., 2010. 2010 Maule earthquake slip correlates with pre-seismic locking of Andean subduction zone, *Nature,* **467,** 198–U184.

Moscoso, E., Grevemeyer, I., Contreras-Reyes, E., Flueh, E., Dzierma, I., Rabbel, W. & Thorwart, M., 2011. Revealing the deep structure and rupture plane of the 2010 Maule, Chile Earthquake (Mw = 8.8) using wide angle seismic data, *Earth planet. Sci. Lett.,* **307,** 147–155.

Oncken, O., Hindle, D., Kley, J., Elger, K., Victor, P. & Schemmann, K., 2006. Deformation of the Central Andean upper plate system: facts, fiction, and constraints for plateau models, in *The Andes: Active Subduction Orogeny,* pp. 3–27, eds Oncken, O., Chong, G., Franz, G., Giese, P., Götze, H.-J., Ramos, V.A., Strecker, M. & Wigger, P., Springer, Berlin.

Pavlis, N., Holmes, S., Kenyon, S. & Factor, J., 2008. An Earth gravitational model to degree 2160: EGM2008, in *Proceedings of General Assembly of the European Geosciences Union,* Vienna, Austria.

Perarnau, M., Alvarado, P. & Saez, M., 2010. Estimación de la estructura cortical de velocidades sísmicas en el suroeste de la Sierra de Pie de Palo, Provincia de San Juan, *Revista de la Aosciación Geológica Argentina,* **67,** 473–480.

Pérez-Gussinyé, M., Lowry, A.R., Phipps Morgan, J. & Tassara, A., 2008. Effective elastic thickness variations along the Andean margin and their relationship to subduction geometry, *Geochem. Geophys. Geosyst.,* **9,** doi:10.1029/2007GC001786.

Ruegg, J. *et al*., 2009. Interseismic strain accumulation measured by GPS in the seismic gap between Constitución and Concepción in Chile, *Phys. Earth planet. Inter.,* **175,** 78–85.
Sallares, V. & Ranero, C.R., 2005. Structure and tectonics of the erosional convergent margin off Antofagasta, north Chile (23 degrees 30‘S), *J. geophys. Res.,* **110,** doi:10.1029/2004JB003418.
Scherwath, M., Contreras-Reyes, E., Flueh, E.R., Grevemeyer, I., Krabbenhoeft, A., Papenberg, C., Petersen, C.J. & Weinrebe, W., 2009. Deep lithospheric structures along the southern central Chile margin from wide-angle P-wave modelling, *Geophys. J. Int.,* **179,** 579–600.
Stern, C.R., 2004. Active Andean volcanism: its geologic and tectonic setting, *Revista Geologica de Chile,* **31,** 161–206.
Tassara, A., 2010. Control of forearc density structure on megathrust shear strength along the Chilean subduction zone, *Tectonophysics,* **495,** 34–47.
Tassara, A., Götze, H.J., Schmidt, S. & Hackney, R., 2006. Three-dimensional density model of the Nazca plate and the Andean continental margin, *J. geophys. Res.,* **111,** doi:10.1029/2005JB003976.
Tassara, A., Swain, C., Hackney, R. & Kirby, J., 2007. Elastic thickness structure of South America estimated using wavelets and satellite-derived gravity data, *Earth planet. Sci. Lett.,* **253,** 17–36.
Uyeda, S. & Kanamori, H., 1979. Back-arc opening and the mode of subduction, *J. geophys. Res.,* **84,** 1049–1061.
Wessel, P. & Smith, W., 1991. Free software helps map and display data, *EOS, Trans. Am. geophys. Un.,* **72,** 441.
Woelbern, I., Heit, B., Yuan, X., Asch, G., Kind, R., Tawackoli, S. & Wilke, H., 2009. Receiver function images from the Moho and the slab beneath the Altiplano and Puna plateaus in the Central Andes, *Geophys. J. Int.,* **177,** 296–308.
Yáñez, G. & Cembrano, J., 2004. Role of viscous plate coupling in the late Tertiary Andean tectonics, *J. geophys. Res.,* **109,** doi:10.1029/2003JB002494.

SUPPORTING INFORMATION

Additional Supporting Information may be found in the online version of this article:

Table S1. The final geometries for the Slab upper surface (SLAB), in the form of an ASCII table that contain the position (longitude, latitude and depth below sea level) of vertices defining each discontinuity across the modelled sections.
Table S2. As Table S1, but for continental lithosphere–asthenosphere boundary (LAB).
Table S3. As Table S1, but for continental Moho (CMH).
Table S4. As Table S1, but for intracrustal discontinuity (ICD).

Please note: Wiley-Blackwell are not responsible for the content or functionality of any supporting materials supplied by the authors. Any queries (other than missing material) should be directed to the corresponding author for the article.